Wetting transitions of ^{4}He on alkali-metal surfaces from density-functional calculations

Francesco Ancilotto, Fabio Faccin, and Flavio Toigo

INFM and Dipartimento di Fisica "G. Galilei," via Marzolo 8, I-35131 Padova, Italy

(Received 22 June 2000)

We have studied the wetting properties of ^{4}He adsorbed on the surface of heavy alkali metals by using a nonlocal free-energy density functional which describes accurately the surface properties of liquid ^{4}He in the temperature range $0 < T < 3$ K. Our results for ^{4}He on the Cs surface give both the temperature dependence of the contact angle and the wetting temperature in good agreement with the experimental findings. For the ^{4}He/Rb system we find that a wetting transition on the Rb surface occurs at $T \sim 1.4$ K, whereas the experiments show either wetting down to $T = 0$ or a wetting transition at $T \sim 0.3$ K. We suggest that this disagreement is due either to an inaccuracy of the fluid-substrate potential used in our calculations or the consequence of substrate roughness, which is known to affect the Rb surface, and whose effect would be to lower the wetting temperature. The sensitivity of the wetting transition to the He-surface potential is stressed for the He/Rb surface, which may justify the controversial experimental findings for this system.

I. INTRODUCTION

The existence and nature of the wetting transition[1] at a temperature above the triple point T_t (and below the critical temperature) is known to be the result of a delicate balance between the interatomic potential acting among the atoms in the liquid and the atom-substrate interaction potential.[2] When the latter dominates, the fluid tends to wet the surface. Because of the extremely weak interaction between He atoms, liquid ^{4}He in contact with almost any substrate spreads to form a continuous film over the surface, so that vapor and substrate are never in contact, thus making ^{4}He the ideal wetting agent.

A remarkable exception to this behavior is found when ^{4}He is adsorbed on heavy alkali metal surfaces: due to the large electron spill-out at their surface, alkali metals provide the weakest adsorption potentials in nature for He atoms. Based on this observation, it was suggested[3,4] that ^{4}He might not wet some heavy alkali metal surfaces. Subsequent experiments have confirmed this remarkable prediction. Actually, experimental evidence that ^{4}He on a Cs substrate (which exerts the weakest attraction to He atoms) exhibits a wetting transition[5-8] at $T_w \approx 2$ K has been collected. The results for ^{4}He on Rb are more controversial, since both a prewetting transition accompanied by complete wetting down to $T = 0$ K,[9] (this is analogous to triple point wetting) and a wetting transition[10] at a nonzero $T_w \approx 0.3$ K have been reported. On the more attractive substrate of potassium, wetting behavior has been observed for all $T > 0$.[11]

Numerical simulations have proven to be a very useful tool to study the wetting properties of fluids. In particular, density-functional (DF) methods[12] have become increasingly popular in recent years because of their ability to describe inhomogeneous fluids and phase equilibria. A comparison with "exact" Monte Carlo simulation results shows that, once the long-range (van der Waals) attractive forces exerted by a surface on the gas atoms are included in the free energy functional, density-functional methods provide a qualitatively (and most often quantitatively) good description of the thermodynamics of gas adsorption on a solid surface and

correctly predict a large variety of phase transitions (wetting, prewetting, layering, etc.).

In particular, a quite accurate description of the $T = 0$ properties of liquid ^{4}He has been obtained within a DF approach by using the energy functional proposed in Ref. 13 and later improved in Ref. 14. This phenomenological functional has been widely tested in a variety of problems involving inhomogeneous phases of liquid ^{4}He (surfaces, droplets, films, etc.),[4,14-17] and is known to give a good description of the $T = 0$ properties of the liquid-vapor interface and also of some properties of liquid ^{4}He on various substrates[18,19] (for a thorough comparison between these and other functionals used to describe liquid ^{4}He at $T = 0$, see Ref. 20). A very remarkable example of success of such theoretical framework is the prediction of the nonwetting behavior of liquid ^{4}He on heavy alkali metals at zero absolute temperature.[4]

In the present work we extend the theory of Refs. 13 and 14 to finite temperatures and apply the functional to the study of wetting properties of ^{4}He adsorbed on alkali metal surfaces. A preliminary account of this work has been presented elsewhere.[21]

A previous attempt to construct a semiempirical finite-temperature density-functional for ^{4}He has been reported in Ref. 22. There, a *local* functional of the density was used (i.e., where the He-He interaction terms correspond to an attractive two-body contact force), with a number of parameters adjusted to guarantee the correct liquid-vapor coexistence. The agreement with the experimental surface tension of liquid ^{4}He at saturated vapor pressure was also imposed by construction. This functional has been applied to the study of the behavior of the liquid-vapor interface thickness as a function of temperature.[22]

It is well known,[23] however, that a local theory gives incorrect fluid structures in situations where the liquid is perturbed on a microscopic scale, as it happens close to a solid substrate. This failure is due to the zero-range nature of the Skyrme interaction used in Ref. 22, which completely neglects the short-range correlations associated with the interatomic potential hard core.

For this reason, in our work we rather use as a starting point for our finite-temperature calculations the *nonlocal*

form of the density functional proposed in Ref. 14, where a more realistic finite-range interactions between He atoms is included. Contrary to what happens with the local functional,[22] this nonlocal functional with parameters fitted to bulk properties provides the correct asymptotic behavior of the surface potential profile without any *ad hoc* prescription, which is a desirable feature in order to properly describe the liquid-vapor interface.

II. METHOD

In the density-functional approach the grand-canonical free energy is considered a functional of the density $\rho(\mathbf{r})$:

$$\Omega_{He}[\rho] = F[\rho] - \mu \int d\mathbf{r}\rho(\mathbf{r}), \tag{1}$$

where μ is the chemical potential and $F[\rho]$ is the free-energy density functional. We propose to write $F[\rho]$ as

$$F = \int f d\mathbf{r}, \tag{2}$$

where

$$f \equiv f_{quant}[\rho] + f_{int}[\rho]. \tag{3}$$

The first term in the right-hand side takes into account the quantum kinetic energy and the free energy density of an ideal Bose gas f_{id}:

$$f_{quant} = \frac{\hbar^2}{2M}(\nabla\sqrt{\rho})^2 + c_4 f_{id} \tag{4}$$

with c_4 an adjustable parameters to be determined by the fitting procedure detailed below.

The ideal-gas contribution f_{id} is given by (see, for instance, Ref. 24):

$$f_{id} = \rho K_B T \ln(z) - \frac{K_B T}{\lambda^3}g_{5/2}(z), \tag{5}$$

where $\lambda \equiv \sqrt{2\pi\hbar^2/MK_BT}$ is the ^{4}He thermal wavelength and the fugacity z is defined as

$$z = \begin{cases} 1 & \text{if } \rho\lambda^3 \geq g_{3/2}(1) \\ z_0 & \text{if } \rho\lambda^3 < g_{3/2}(1), \end{cases}$$

where z_0 is the root of the equation $\rho\lambda^3 = g_{3/2}(z)$. In the above equations, $g_n(z) \equiv \Sigma_{l=1}^{\infty} z^l/l^n$.

As in the original $T=0$ functional,[14] f_{int} accounts for He-He interactions (in a Hartree-like fashion) and for correlations effects:

$$f_{int}[\rho(\mathbf{r})] = \frac{1}{2}\int d\mathbf{r}' \rho(\mathbf{r})\rho(\mathbf{r}')V_l(|\mathbf{r}-\mathbf{r}'|)$$

$$+ \frac{c_2}{2}\rho(\mathbf{r})[\bar{\rho}(\mathbf{r})]^2 + \frac{c_3}{3}\rho(\mathbf{r})[\bar{\rho}(\mathbf{r})]^3$$

$$- \frac{\hbar^2}{4M}\alpha_s\int d\mathbf{r}' G(|\mathbf{r}-\mathbf{r}'|)\left(1-\frac{\rho(\mathbf{r})}{\rho_{0s}}\right)$$

$$\times \nabla\rho(\mathbf{r})\nabla\rho(\mathbf{r}')\left(1-\frac{\rho(\mathbf{r}')}{\rho_{0s}}\right). \tag{6}$$

The first term contains a two-body He-He pair potential $V_l(r)$ (of the Lennard-Jones type, with $\epsilon = 10.22$ K and $\sigma = 2.556$ Å) screened at distances shorter than a characteristic length h_l ($V_l = 0$ for $r < h_l$), while the second and third terms contain $\bar{\rho}(\mathbf{r})$, i.e., the average of the density over a sphere of radius h_l, and account for the increasing contribution of the hard-core He-He repulsion when the density is increased. The last term contains the gradient of the density at different points and corresponds to a nonlocal correction to the kinetic energy.

We remark at this point that the quantum kinetic energy term appearing in Eq. (4) (as well as in other phenomenological density-functional theories used to describe inhomogeneous ^{4}He) is derived from the *total* density $\rho(\mathbf{r})$. However, as discussed in Ref. 25, a complete density-functional theory of Bose-condensed liquids would rather involve functionals of both the local density $\rho(\mathbf{r})$ and the local order parameter $\Phi(\mathbf{r}) = \sqrt{\rho_c(\mathbf{r})}$, $\rho_c(\mathbf{r})$ being the local condensate density. In particular, the counterpart of the first term in Eq. (4) would be proportional to $(\nabla\sqrt{\rho_c})^2$. A rationalization of why the simplified form of the density functional used here (and in all other applications of DF theory to liquid ^{4}He as well) leads to a satisfactory description of the surface can be traced to the fact that the two quantum kinetic energy terms coincide in the low density surface region, which is important for the interface problems, where $\rho_c(\mathbf{r}) \sim \rho(r)$.[25]

In the $T=0$ functional,[14] the free parameters h_l, c_2, and c_3 were adjusted in order to reproduce the experimental values of the density, of the energy per atom, and of the compressibility for bulk liquid ^{4}He at zero pressure, while the width l_G of the Gaussian function G and the parameters α_s and ρ_{0s} in Eq. (6) were adjusted to reproduce the overall shape of the experimental static response function of bulk liquid ^{4}He. For a detailed description of the various terms in Eq. (6) we refer the reader to Ref. 14.

We follow the same philosophy at finite temperatures, i.e., we consider the free energy density of a uniform system ($\rho = $ constant) as given in Eqs. (4) and (6) :

$$f \equiv F/V = \frac{1}{2}b\rho^2 + \frac{1}{2}c_2\rho^3 + \frac{1}{3}c_3\rho^4 + c_4 f_{id}(\rho,T), \tag{7}$$

where

$$b = \int d\mathbf{r}V_l(\mathbf{r}) = 4\pi\int_{h_l}^{\infty} dr\, r^2 V_l(\mathbf{r}) \tag{8}$$

and minimize the grand potential with respect to ρ to get the chemical potential

$$\mu(\rho,T) \equiv \frac{\partial f}{\partial\rho} = b\rho + \frac{3}{2}c_2\rho^2 + \frac{4}{3}c_3\rho^3 + c_4\mu_{id} \tag{9}$$

and the pressure

$$P(\rho,T) \equiv \rho\mu - f = \frac{1}{2}b\rho^2 + c_2\rho^3 + c_3\rho^4 + c_4 P_{id}. \tag{10}$$

The ideal-gas contributions to the chemical potential and pressure in the above equations are $\mu_{id} = K_B T \ln(z)$ and $P_{id} = K_B T g_{5/2}(z)/\lambda^3$.

TABLE I. Density functional coefficients.

T(K)	ρ_l (Å^{-3})	ρ_v (Å^{-3})	b (K Å^3)	c_2 (K Å^6)	c_3 (K Å^9)	c_4	h_l (Å)
0.0	0.0218354	0.0	-719.2435	-24258.88	1865257	0.0	2.19035
0.4	0.0218351	0.441987(-11)	-714.2174	-24566.29	1873203	0.98004	2.18982
0.6	0.0218346	0.452619(-8)	-705.1319	-25124.17	1887707	0.99915	2.18887
0.8	0.0218331	0.133640(-6)	-690.4745	-26027.12	1911283	0.99548	2.18735
1.2	0.0218298	0.495337(-5)	-646.5135	-28582.81	1973737	0.99666	2.18287
1.4	0.0218332	0.147990(-4)	-625.8123	-29434.03	1984068	0.99829	2.18080
1.6	0.0218453	0.346234(-4)	-605.9788	-30025.96	1980898	1.00087	2.17885
1.8	0.0218703	0.684096(-4)	-593.8289	-29807.56	1945685	1.00443	2.17766
2.0	0.0219153	0.119400(-3)	-600.8313	-27850.96	1847407	1.00919	2.17834
2.1	0.0219500	0.151732(-3)	-620.9129	-25418.15	1747494	1.01156	2.18032
2.2	0.0219859	0.188202(-3)	-619.2016	-25096.68	1720802	1.01436	2.18015
2.4	0.0218748	0.275044(-3)	-609.0757	-26009.98	1747943	1.02130	2.17915
2.6	0.0217135	0.383550(-3)	-634.0664	-23790.66	1670707	1.02770	2.18162
2.8	0.0215090	0.516536(-3)	-663.9942	-21046.37	1574611	1.03429	2.18463
3.0	0.0212593	0.676814(-3)	-673.6543	-20022.76	1535887	1.04271	2.18562

If ρ_v and ρ_l are the densities of vapor and liquid ^{4}He at saturated vapor pressure at a given temperature T, then at coexistence the equilibrium conditions

$$\mu(\rho_l,T)=\mu(\rho_v,T) \qquad (11)$$

and

$$P(\rho_l,T)=P(\rho_v,T) \qquad (12)$$

must be satisfied.

By requiring that equalities (11) and (12) are satisfied when the experimental values of ρ_v and ρ_l are inserted into Eqs. (9) and (10) and, moreover, that the common value of the chemical potentials in Eq. (11) is equal to the experimental value at the same temperature,[26]

$$\mu(\rho_l,T)=\mu^{expt}(T), \qquad (13)$$

we get three equations relating the four adjustable coefficients c_2, c_3, c_4, and b.

As a fourth equation necessary to determine them completely at any temperature of interest we impose that the calculated isothermal compressibility, $1/K \equiv \rho(\partial P/\partial \rho)$, reproduces its corresponding experimental value:

$$K(\rho_l,T)=K^{expt}(T). \qquad (14)$$

The fit has been carried out in the region $0 < T < 3$ K, which is the most interesting for the wetting properties of ^{4}He we want to investigate. Once $b(T)$ has been obtained by solving the system of four equations described above, the quantity $h_l(T)$ can be easily calculated by numerically inverting the relation (8). In this way all coefficients entering the functional (6) are determined. The calculated coefficients are shown, for some selected temperatures, in Table I.

The three additional parameters entering the gradient-dependent term in Eq. (6) (l_G, α_s, and ρ_{0s}) may be fixed to reproduce the static response function of bulk liquid ^{4}He. Since the experimental information for the temperature dependence of this quantity is very limited, for all temperatures in our calculations we used the same values as those of the

$T=0$ functional,[14] fitted by Dalfovo *et al.*[14] to the only existing experimental measurements, performed at $T=1.1$ K.

We wish to stress at this point that all unknown coefficients entering the free energy density functional of pure ^{4}He are fitted to bulk properties, i.e., to properties of uniform systems. To include the interaction with the substrate, we use a binding potential $V_s(z)$ which describes the interaction between the alkali metal, occupying the half space $z \leqslant 0$, and one ^{4}He atom located at a distance z above the ideally flat surface.

The physisorption potential $V_s(z)$ is taken in the form originally proposed in Ref. 27, i.e., as a sum of a Hartree-Fock repulsion and a van der Waals attraction. Both terms are parametrized with a set of coefficients. Very reliable values for the parameters entering $V_s(z)$ and describing the interaction of ^{4}He and other noble-gas atoms with alkali substrates have been calculated from first principles.[28] These potentials have been used to calculate the wetting properties of rare gases (other than He) on alkali metal surfaces[29] and also the $T=0$ profile of a droplet on the Cs surface,[19] and found to give predictions in reasonable agreement with experiments for all these systems.

The total free energy functional for ^{4}He interacting with the substrate is thus

$$\Omega[\rho(\mathbf{r})]=\Omega_{He}[\rho(\mathbf{r})]+\int d\mathbf{r}\rho(\mathbf{r})V_s(z). \qquad (15)$$

According to density-functional theory, the equilibrium density profile $\rho(\mathbf{r})$ of the fluid in the presence of the substrate can be determined by applying the variational principle

$$\delta\Omega/\delta\sqrt{\rho(\mathbf{r})}=0 \qquad (16)$$

to get the Euler-Lagrangian equation

$$\left(-\frac{\hbar^2}{2M}\nabla^2+U[\rho(\mathbf{r})]+V_s(z)\right)\sqrt{\rho(\mathbf{r})}=\mu\sqrt{\rho(\mathbf{r})}, \qquad (17)$$

where the effective potential U is defined as $U[\rho(\mathbf{r})] \equiv \delta \int [c_4 f_{id} + f_{int}] d\mathbf{r}' / \delta \rho(\mathbf{r})$ and the value of the chemical potential μ is fixed by the normalization condition

$$\int d\mathbf{r}\rho(\mathbf{r}) = N, \tag{18}$$

N being the total number of ^{4}He atoms.

III. RESULTS AND DISCUSSION

Wetting or nonwetting is determined by surface tension balancing. The intersection of a macroscopic liquid droplet with a solid planar substrate can be characterized by the contact angle Θ: it goes to zero as T approaches T_w and remains zero at all higher temperatures, where the liquid wets the substrate. Below the wetting temperature, the contact angle is determined by balancing the forces acting along the contact line and depends on the interfacial tensions σ_{ij} between each pair of coexisting phases through Young-Dupre's equation

$$\cos \Theta = \frac{\sigma_{sv} - \sigma_{sl}}{\sigma_{lv}}. \tag{19}$$

The subscripts l, v, and s identify the liquid, vapor, and solid, respectively. We have calculated the interfacial tensions σ_{ij} entering Eq. (19) at selected values of T by using the density-functional method described in the previous section.

We first studied the liquid-vapor interface of ^{4}He by solving Eq. (17) (with $V_s \equiv 0$) with the appropriate boundary conditions, corresponding to a planar liquid film in equilibrium with its own vapor. In this case the solution depends only on the coordinate z normal to the surface, and provides the equilibrium density profile $\rho(z)$.

Our calculations are performed within a region of length z_m. In a typical calculation we start by considering an initial density configuration $\rho_0(z)$ which mimics a liquid film in contact with its own vapor (usually we choose a double-stepped profile with liquidlike density at the center and much lower values at the boundaries). This defines an areal density $n \equiv N/A = \int_0^{z_m} \rho_0(z) dz$, and an initial effective potential U to be inserted into the minimization Eq. (17) which must be solved iteratively to self-consistency. At any step of the self-consistency cycle, the solution $\rho(z)$ is normalized to the value of the areal density n: $\int_0^{z_m} dz \rho(z) = n$. The calculated chemical potential μ corresponding to the chosen value of n is then the eigenvalue of Eq. (17) at self-consistency.

By increasing the slab thickness and z_m to allow that both the liquid and vapor phases develop a bulk behavior (i.e., constant densities) far from the liquid-vapor interface, the chemical potential gets values slightly below, but very close (1–2 mK in a typical calculation), to the bulk coexistence value: these slight differences are expected due to the finite size of the system, and decrease extremely slowly by increasing z_m beyond a certain length. This way of proceeding is useful in determining the minimum cell dimension and film thickness which allow for this bulk behavior, and thus give a converged value for the surface tensions.

This (i.e., fixing the areal density and calculating μ) is also the approach that one must follow in order to determine
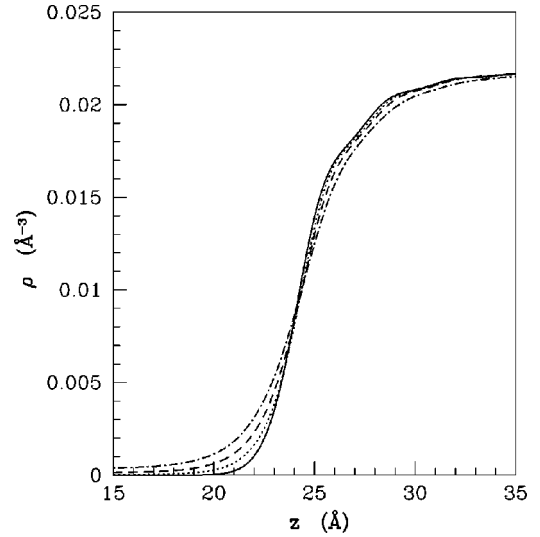

FIG. 1. Calculated ^{4}He density profile near the liquid-vapor interface. Solid line: $T = 0$ K; dotted line: $T = 1.5$ K; dashed line: $T = 2$ K; dash-dotted line: $T = 2.5$ K.

the wetting behavior off coexistence, where one needs the chemical potential as a function of n to study the occurrence of prewetting transitions, etc.

If one is only interested at the system behavior at coexistence, however, one could alternatively fix from the start the value of the chemical potential at its bulk value and proceed with the self-consistent minimization without preserving the areal density. For sufficiently large cells (i.e., when finite-size effects may be considered negligible) the two approaches give the same results. Despite the fact the latter approach is more efficient (i.e., a smaller number of steps is required for the minimization of the functional), we have chosen to follow the first scheme, which has the advantage of providing a useful check on the overall consistency of the calculations (fit of the parameters and minimization algorithms). In fact, the chemical potential and the liquid and vapor densities far from the interface region, obtained as an output of the calculation, should reproduce the experimental values used in the fit. We verified, in any case, that the two approaches give values of the surface tension, which is the more sensitive quantity to the details of the calculations, with relative differences not exceeding 0.1–0.2%.

Rather large values of z_m and of the film thickness t_f are necessary in the present case for well converged calculations (typically $z_m \sim 200$ Å and $t_f \sim 150$ Å), in order to let the system spontaneously reach (i) the liquid bulk density in the interior of the film and (ii) the vapor bulk density in the region outside the film. In Fig. 1 we show some selected density profiles close to the liquid-vapor interface. A detailed analysis of the resulting density profiles shows that the width of the interface increases monotonically with temperature. A comparison of our results with those obtained in Ref. 22 indicates also that the thickness of the liquid-vapor interface, at a given temperature, is slightly smaller than that obtained from the zero-range functional of Ref. 22. This result is also in agreement with the behavior found at $T = 0$ (see, for instance, Fig. 4 in Ref. 20).

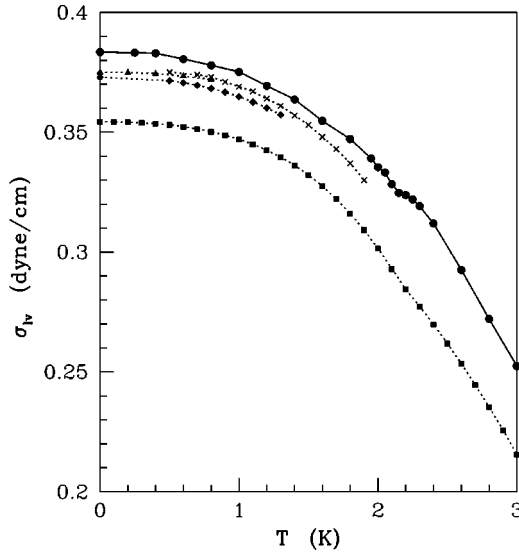From the calculated equilibrium density profiles one can directly compute the liquid-vapor surface tension σ_{lv}, from

FIG. 2. Surface tension of liquid ^{4}He. Dots: calculated σ_{lv}; squares, diamonds, triangles, and crosses show the experimental results from Refs. 30–32, and 33, respectively. Lines are only a guide to the eye.

FIG. 3. Equilibrium density profiles used to calculate σ_{sl} (upper curve, with solid line), and σ_{sv} (lower curve, with dotted line), respectively.

the definition $\sigma = (\Omega + PV)/A$. Here P is the saturated vapor pressure at temperature T, V is the volume of the system, and A is the surface area. For the one-dimensional problem considered here, one can write

$$\sigma = (1/2) \left(\int_0^{z_m} f(\rho(z)) dz - \mu \int_0^{z_m} \rho(z) dz + P z_m \right). \quad (20)$$

The pressure P can be conveniently calculated from the definition $P = [\mu\rho_v - f(\rho_v)] = [\mu\rho_l - f(\rho_l)]$, ρ_v and ρ_l being the experimental densities for bulk liquid and vapor, respectively. A factor $1/2$ appears in the previous equation to account for the two free surfaces delimiting the liquid film in our ''slab'' calculations.

The dependence of the liquid-vapor surface tension of ^{4}He on temperature has been extensively investigated in the past. Surprisingly, the absolute value of σ_{lv} at $T=0$ remains poorly known: predictions from different groups give values for $\sigma_{lv}(0)$ differing by up to 6%.[30–33] Our calculated values are shown in Fig. 2, where they are compared with the available experimental data. The overall agreement is quite satisfactory, given the fact that our functional has been fitted to reproduce ^{4}He bulk properties only. Note also that the kink (barely) visible in the experimental data at the temperature corresponding to the λ point $T_\lambda = 2.17$ K appears also in our calculated σ_{lv} and reflects similar kinks appearing close to T_λ in the bulk quantities (density, chemical potential, and compressibility) used to fit the coefficients entering the free energy (3).

We next turn to the problem of liquid ^{4}He in the presence of a solid surface. The two additional surface tensions σ_{sv} and σ_{sl} required to obtain the contact angle Θ from Eq. (19) are calculated within our density-functional approximation by using different boundary conditions from those used to calculate σ_{lv}. We confine the fluid between two parallel surfaces, separated by a distance large enough to avoid any compression effect. The two surfaces act on the fluid with
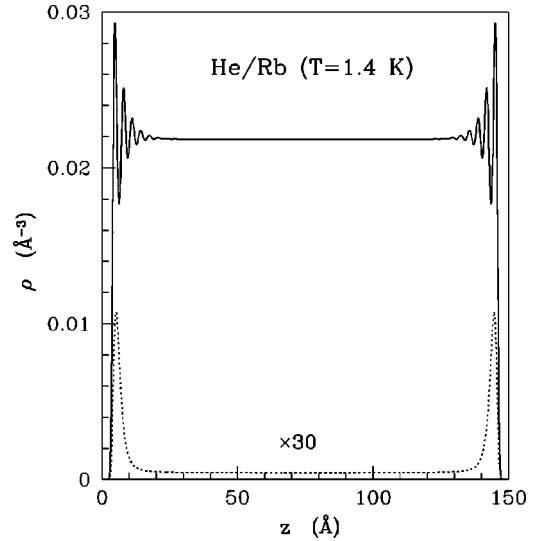
the external potential $V_s(z)$ appropriate to the alkali metal substrate. For selected values of the temperature T, we get the structure of the solid-vapor and solid-liquid interfaces by minimizing the grand-potential (15) subject to the additional constraint that the density in a large region between the two surfaces (where bulk behavior is expected) is equal respectively to ρ_v and ρ_l. The corresponding surface excess energies per unit area $\sigma = (\Omega + PV)/(2A)$ are the solid-vapor σ_{sv} and the solid-liquid σ_{sl} surface tensions. Of course the distance between the two confining surfaces must be such that the calculated values of σ_{sv} and σ_{sl} do not change by further increasing their separation. We show in Fig. 3 the equilibrium density profiles of ^{4}He confined between two Rb surfaces, at $T=1.4$ K. The solid line shows the density for the liquid phase confined between the surfaces, the dotted line (which is rescaled for clarity by a factor 30) shows instead the vapor density profile. The profiles shown correspond to the areal densities $n_c = 3.13$ Å^{-2} and $n_c = 4.60 \times 10^{-3}$ Å^{-2}, respectively. Note the oscillations of the liquid density close to the surface, due to close-packing effects. We have checked, by means of similar calculations with different cell sizes, that at least 150 Å must separate the two attractive surfaces so that the two fluid-solid interfaces are effectively decoupled and the calculation gives a converged value for the surface tensions σ_{sl} and σ_{sv}.

According to Eq. (19), wetting of a surface occurs at a temperature T_w such that

$$\sigma_{sv} - \sigma_{sl} = \sigma_{lv}. \quad (21)$$

In Fig. 4 we show the behavior of the two sides of Eq. (21) as a function of temperature, for three different alkali surfaces. A common feature of the curves for $\sigma_{sv} - \sigma_{sl}$ shown in Fig. 4 is their rather weak temperature dependence, as indeed observed in experiments.[34] Moreover, σ_{sv} is always much smaller than σ_{sl}, as can be seen in Table II, where the two surface tensions σ_{sv} and σ_{sl} for ^{4}He on Cs are shown separately for some selected temperatures. Our predicted wetting temperature for Cs, $T_w \sim 2.1$ K, is in good
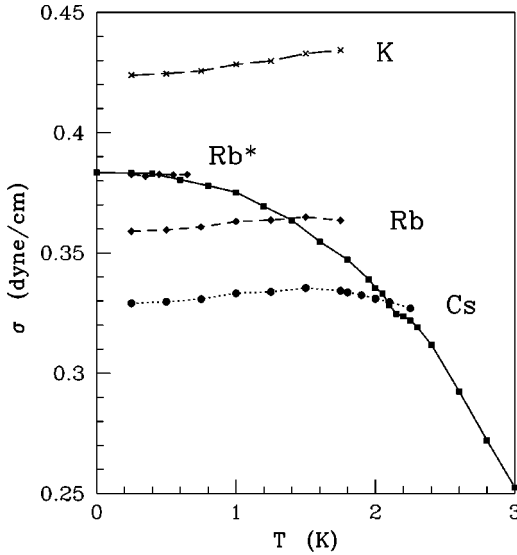
FIG. 4. Calculated surface tensions for the ^{4}He/alkali systems. Squares: σ_{lv}; dots, diamonds, and crosses show $(\sigma_{sv} - \sigma_{sl})$ for ^{4}He/Cs, ^{4}He/Rb, and ^{4}He/K, respectively. The set of points labeled Rb* are obtained by using a modified ^{4}He/Rb surface interaction, as explained in the text. Lines are only a guide to the eye.
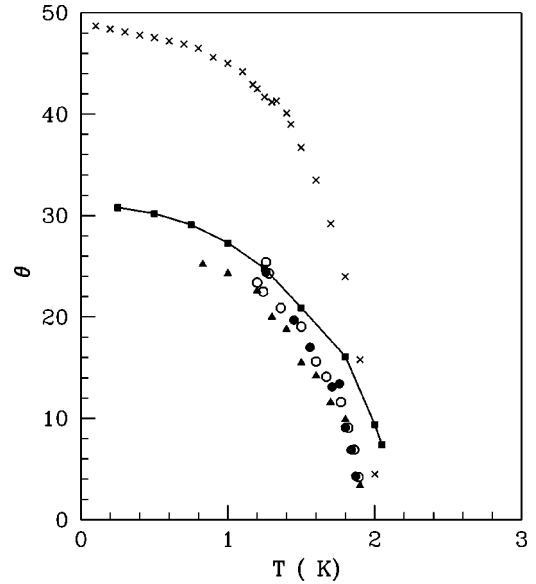

FIG. 5. Temperature dependence of the ^{4}He/Cs contact angle: squares: this work; triangles, dots, and crosses show the experimental results from Refs. 34, 36, and 8, respectively. Open and filled dots, from Ref. 36, refer to two differently prepared Cs surfaces.

agreement with the experimental value $T_w \sim 2$ K. Also in the case of ^{4}He on K our calculated results shown in Fig. 4 agree with experiments,[9] indicating wetting at any $T > 0$. On the contrary, for Rb our calculations predict a wetting temperature $T_w \sim 1.4$ K, in marked disagreement with the experimental findings which show instead either complete wetting down to $T = 0$,[9] or a wetting transition at $T_w \approx 0.3$ K.[10]

We remark that the portion of curves above the σ_{lv} are strictly speaking unphysical, since in that region the spreading pressure $\sigma_{lv} - \sigma_{sv} + \sigma_{sl}$ is negative, implying thermodynamic instability. We can actually get these states because we are imposing the additional constraint that the value of the density in the middle of the cell does coincide with the bulk density, thus enforcing the stability of an otherwise unstable state. If this constraint is relaxed, the final configuration will be either a wet or incomplete wet profile, depending on whether T is above or below T_w.

We show in Fig. 5 the temperature dependence of the contact angle for the ^{4}He/Cs system as obtained from our calculations, together with the available experimental data. Although the equilibrium contact angle is a well defined thermodynamic quantity, measurements of this quantity invariably show a strong hysteretic behavior, i.e., the measured value of the contact angle depends on whether the contact

line is advancing or receding. For relatively homogenous surfaces, however, it has been shown that the advancing contact angle is a good measure of the equilibrium contact angle, so we compare our results with the experimental values for that quantity. The contact angle for ^{4}He on Cs surfaces has been measured by different groups in recent years by using different techniques.[8,34–36] In Refs. 35 and 36 the contact angle is measured by direct visual inspection of macroscopic droplets of superfluid ^{4}He on a Cs surface. In Ref. 34 the contact angle is obtained by means of direct optical measurements using interferometric techniques, whereas in Ref. 8 it is measured, much more indirectly, from the reduction in pressure due to capillarity, when an array of parallel tungsten plates coated with Cesium are immersed into liquid ^{4}He. Our results are compared in Fig. 5 with the aforementioned experimental data. The overall agreement with the results from Refs. 34–36 is satisfying, although a strong discrepancy exists with the data of Ref. 8.

At variance with the overall satisfactory quantitative agreement we get for the ^{4}He/Cs system, our predictions seems to be wrong for the ^{4}He/Rb system. We believe that this disagreement is probably due to the fact that our assumptions of a rigid and planar substrate are far from being satisfied in this case. Impurities or roughness, in fact, are always present on the surface, as indicated by the strong hysteretic behavior of the contact angle observed in all experiments when studying advancing or receding contact lines. This condition may be particularly severe in the case of the Rb surface, where defects and roughness are known to be present to a larger extent than on the surface of Cs.

The heterogeneity of the substrate is known to promote wetting, i.e., leads to values of $\sigma_{sv} - \sigma_{sl}$ higher than for an ideal substrate. In the case of ^{4}He on Rb, as apparent from Fig. 4, an increase of $\sigma_{sv} - \sigma_{sl}$ would shift the wetting temperature towards lower values, as indeed found in experiments.

The characterization of the wetting behavior of superfluid

TABLE II. Surface tensions (in dyne/cm) for the ^{4}He/Cs system.

T(K)	σ_{sv}	σ_{sl}
1.00	−0.0003	−0.3335
1.25	−0.0011	−0.3349
1.50	−0.0027	−0.3381
1.75	−0.0053	−0.3396
2.00	−0.0091	−0.3401
2.10	−0.0109	−0.3406

helium on rough surfaces is a very difficult task. The quality of the substrates used in the experiments cannot be determined at lengthscales smaller than optical wavelengths. The theoretical description of the effects of heterogeneities is also challenging. Only few theoretical results are available on the effect of microscopic disorder[37,38] on the wetting properties of fluids adsorbed on weakly attractive surfaces.

The effect of model disorder (on an atomic scale) on the wetting properties of Ne on the Mg surface has been studied by Curtarolo *et al.*[37] One interesting conclusion contained in this paper is that roughness destroy the discontinuous nature of the wetting transition, even if a trace of discontinuities remain in the calculated isotherms.

In Ref. 38 a Lennard-Jones fluid and its wetting properties on molecularly rough surfaces have been studied by using molecular dynamics. Contrary to the conventional belief that surface roughness reduces the contact angle thus making it easier to wet a rough surface than a smooth one, the surprising conclusion of this work is that the contact angle is larger for the rough surface than for the smooth one.

In order to have further insight into this important issue, we are currently investigating the effect of a realistic distribution of microscopic disorder on the wetting transition of ^{4}He on the Rb surface within the density-functional approach described here.[39]

An alternative explanation for the disagreement with the experiments for the ^{4}He/Rb system is that the He-Rb surface potential used in our calculations is inaccurate. Our overestimate of the wetting temperature would be a sign, in this case, that the calculated potential is slightly less attractive than required to provide a result closer to the experimental one.

We have thus tried a modified He/Rb surface interaction by changing slightly the two parameters entering the repulsive part of the *ab initio* potential $V_s(z)$ describing the He-surface interaction. The modified potential, has a minimum of depth $D = 0.661$ meV located at $z_{min} = 8.46\, a_0$, to be compared with the values $D = 0.629$ meV and $z_{min} = 8.60\, a_0$ obtained with the original parameters. Such a tiny variation in the adsorption potential ($\sim 5\%$ increase in the potential well depth) has quite a large effect on the He/Rb wetting temperature, as can be judged from the curve labeled Rb* in Fig. 4. With this modified potential the wetting transition moves very close to $T = 0$, as in the experiments. Interestingly, in this case the curve $-\sigma_{sl}(T)$ almost coincides with the curve $\sigma_{lv}(T)$ for a range of T values, between 0 and 0.3–0.4 K (at such temperatures the contribution σ_{sv} is negligible in our approximations). This could provide a reason for the different experimental estimates of the wetting temperature (either $T = 0$ or $T \sim 0.3$–0.4 K) by different groups: in the region where the two curves almost overlap their slope is very small, and thus small variations in the quality of the substrate may result in rather different wetting temperatures. Moreover, this could also suggest a different character of the wetting transition for He/Rb, since similar slopes in $-\sigma_{sl}(T)$ and $\sigma_{lv}(T)$ imply a small discontinuity in $d\cos(\Theta)/dT$, i.e., a quasicontinuous transition.

Finally, we observe that in principle one could use an alternative approach to study the wetting transition which does not require the explicit calculation of the contact angle, i.e., by varying the temperature of the system and looking at the occurrence of density profiles where different interfaces (liquid-solid, liquid-vapor or solid-vapor) are simultaneously present (see, for instance, Ref. 40). One could then infer wetting vs partial wetting behavior from the occurrence of either symmetric (two solid-liquid plus two liquid-vapor interfaces) or nonsymmetric (one solid-liquid plus liquid-vapor plus vapor-solid interfaces) profiles.

This is not, however, a very efficient way of looking for the wetting transitions for several reasons. First of all, it may takes quite a long time to reach, starting from some arbitrary density profile, the equilibrium configurations where multiple interfaces are present. It has been also found[40] that, due to finite-size effects, an asymmetric profile which is the signal of incomplete wetting is intrinsically more stable than a symmetric profile (complete wetting), even at the thermodynamic conditions where wetting should occur. Even if these size effects can be made negligible, as a consequence of the first-order nature of the wetting transition a large hysteresis in the shape of the density profiles with temperature is expected, implying for instance a large interval of temperatures where both symmetries may be observed, thus making difficult to locate the wetting temperature.

IV. SUMMARY

We have extended to finite temperatures the nonlocal density functional proposed in recent years to describe the ^{4}He properties at $T = 0$,[13,14] and studied the wetting behavior of ^{4}He adsorbed on alkali metal surfaces. The density-functional depends on a number of temperature-dependent phenomenological parameters which are adjusted to reproduce *bulk* experimental properties of liquid ^{4}He at saturated vapor pressure. We find that the resulting functional describes accurately the properties of the liquid-vapor interface of the free ^{4}He surface. In the presence of an external potential simulating a planar, solid surface whose binding properties reproduce those of alkali metal surfaces, it also accurately reproduces the properties of the ^{4}He/Cs system, giving the temperature dependence of the contact angle in good agreement with experiments. The contact angle vanishes at $T \sim 2.1$ K, in agreement with the experimental measure for the wetting temperature, $T \sim 2$ K. For ^{4}He on a K surface, we find wetting at all nonzero temperatures, as found also in experiments. For ^{4}He on the Rb surface, however, our calculations fail to reproduce quantitatively the experiments, indicating a wetting transition at $T \sim 1.4$ K. The discrepancy with experiments could be either due to our neglect of surface inhomogeneities, which are known to be present on this surface to a larger extent than on a Cs surface, or to some inaccuracy in the theoretical determination of the surface-adatom potential used in our calculations. If this is the case, our results indicate that the correct potential should be slightly more attractive than currently believed.

[1] J.W. Cahn, J. Chem. Phys. **66**, 3667 (1977).

[2] See, for example, S. Dietrich, in *Phase Transitions and Critical Phenomena*, edited by C. Domb and J. Lebowitz (Academic Press, San Diego, 1988) Vol. 12; B. Evans and M.H.W. Chan, Phys. World **9(4)**, 48 (1996).

[3] E. Cheng, M.W. Cole, W.F. Saam, and J. Treiner, Phys. Rev. Lett. **67**, 1007 (1991).

[4] E. Cheng, M.W. Cole, W.F. Saam, and J. Treiner, Phys. Rev. B **46**, 13 967 (1992).

[5] P. Taborek and J.E. Rutledge, Phys. Rev. Lett. **68**, 2184 (1992); J.E. Rutledge and P. Taborek, *ibid.* **69**, 937 (1992).

[6] P.J. Nacher and J. Dupont-Roc, Phys. Rev. Lett. **67**, 2966 (1991).

[7] K.S. Ketola, S. Wang, and R.B. Hallock, Phys. Rev. Lett. **68**, 201 (1992); R.B. Hallock, J. Low Temp. Phys. **101**, 31 (1995).

[8] J. Klier, P. Stefanyi, and A.F.G. Wyatt, Phys. Rev. Lett. **75**, 3709 (1995); J. Klier and A.F.G. Wyatt, J. Low Temp. Phys. **110**, 919 (1998).

[9] J.A. Phillips, D. Ross, P. Taborek, and J.E. Rutledge, Phys. Rev. B **58**, 3361 (1998).

[10] A.F.G. Wyatt, J. Klier, and P. Stefanyi, Phys. Rev. Lett. **74**, 1151 (1994); J. Klier and A.F.G Wyatt, J. Low Temp. Phys. **113**, 817 (1998).

[11] J.A. Phillips, P. Taborek, and J.E. Rutledge, J. Low Temp. Phys. **113**, 829 (1998).

[12] R. Evans, Adv. Phys. **28**, 144 (1979).

[13] J. Dupont-Roc, M. Himbert, N. Pavloff, and J. Treiner, J. Low Temp. Phys. **81**, 31 (1990).

[14] F. Dalfovo, A. Lastri, L. Pricaupenko, S. Stringari, and J. Treiner, Phys. Rev. B **52**, 1193 (1995).

[15] F. Dalfovo, Z. Phys. D: At., Mol. Clusters **29**, 61 (1994); M. Casas, F. Dalfovo, A. Lastri, Ll. Serra, and S. Stringari, *ibid.* **35**, 67 (1995); A. Lastri, F. Dalfovo, L. Pitaevskii, and S. Stringari, J. Low Temp. Phys. **98**, 227 (1995); F. Dalfovo, A. Fracchetti, A. Lastri, L. Pitaevskii, and S. Stringari, Phys. Rev. Lett. **75**, 2510 (1995); J. Low Temp. Phys. **104**, 367 (1996).

[16] M. Barranco and E.S. Hernandez, Phys. Rev. B **49**, 12 078 (1994).

[17] F. Ancilotto, E. Cheng, M.W. Cole, and F. Toigo, Z. Phys. B: Condens. Matter **98**, 323 (1995).

[18] F. Ancilotto and F. Toigo, Phys. Rev. B **50**, 12 820 (1994).

[19] F. Ancilotto, A.M. Sartori, and F. Toigo, Phys. Rev. B **58**, 5085 (1998).

[20] L. Szybisz, Eur. Phys. J. B **14**, 733 (2000).

[21] F. Ancilotto, F. Faccin, and F. Toigo, *Proceedings of the 14th Symposium of Thermophysical Properties*, Boulder, Colorado, June 25-30, 2000, Fluid Phase Equilibria (to be published).

[22] A. Guirao, M. Centelles, M. Barranco, M. Pi, A. Polls, and X. Vinas, J. Phys.: Condens. Matter **4**, 667 (1992).

[23] R. Evans, *Fundamentals of Inhomogeneous Fluids*, edited by D. Henderson (Dekker, New York, 1992), Chap. 3.

[24] R. K. Pathria, *Statistical Mechanics* (Pergamon, Oxford, 1972).

[25] A. Griffin and S. Stringari, Phys. Rev. Lett. **76**, 259 (1996).

[26] J. Maynard, Phys. Rev. B **14**, 3868 (1976).

[27] E. Zaremba and W. Kohn, Phys. Rev. B **15**, 1769 (1977).

[28] A. Chizmeshya, M.W. Cole, and E. Zaremba, J. Low Temp. Phys. **110**, 677 (1998).

[29] F. Ancilotto and F. Toigo, Phys. Rev. B **60**, 9019 (1999).

[30] M. Ino, M. Suzuki, and A.J. Ikushima, J. Low Temp. Phys. **61**, 155 (1985).

[31] K.R. Atkins and Y. Narahara, Phys. Rev. **138**, A437 (1965).

[32] K.N. Zinoveva and S.T. Bolarev, Zh. Éksp. Teor. Fiz. **56**, 1089 (1969) [Sov. Phys. JETP **29**, 585 (1969)].

[33] P. Roche, G. Deville, N.J. Appleyard, and F.I.B. Williams, J. Low Temp. Phys. **106**, 565 (1977).

[34] E. Rolley and C. Guthmann, J. Low Temp. Phys. **108**, 1 (1997).

[35] D. Ross, J.E. Rutledge, and P. Taborek, Science **278**, 664 (1997).

[36] J.E. Rutledge, D. Ross, and P. Taborek, J. Low Temp. Phys. **113**, 811 (1998).

[37] S. Curtarolo, G. Stan, M.W. Cole, M.J. Bojan, and W.A. Steele, Phys. Rev. E **59**, 4402 (1999).

[38] J.Z. Tang and J.G. Harris, J. Chem. Phys. **103**, 8201 (1995).

[39] S.M. Gatica, F. Ancilotto, and F. Toigo (unpublished).

[40] J.H. Sikkenk, J. O. Indekea, J. M. J. Vanleeuwen, E. O. Vossnack, and A. N. Bakker, J. Stat. Phys. **52**, 23 (1988).